



**HAL**  
open science

# Measurement of the local water content of an epoxy adhesive by fiber optic sensor based on Fresnel reflection

Romain Grangeat, Marion Girard, Cyril Lupi, Dominique Leduc, Frédéric Jacquemin

## ► To cite this version:

Romain Grangeat, Marion Girard, Cyril Lupi, Dominique Leduc, Frédéric Jacquemin. Measurement of the local water content of an epoxy adhesive by fiber optic sensor based on Fresnel reflection. Mechanical Systems and Signal Processing, 2020, 141, pp.106439. 10.1016/j.ymssp.2019.106439 . hal-04033230

**HAL Id: hal-04033230**

**<https://hal.science/hal-04033230>**

Submitted on 17 Mar 2023

**HAL** is a multi-disciplinary open access archive for the deposit and dissemination of scientific research documents, whether they are published or not. The documents may come from teaching and research institutions in France or abroad, or from public or private research centers.

L'archive ouverte pluridisciplinaire **HAL**, est destinée au dépôt et à la diffusion de documents scientifiques de niveau recherche, publiés ou non, émanant des établissements d'enseignement et de recherche français ou étrangers, des laboratoires publics ou privés.



Distributed under a Creative Commons Attribution - NonCommercial - NoDerivatives 4.0 International License

# Measurement of the local water content of an epoxy adhesive by fiber optic sensor based on Fresnel reflection

Romain Grangeat<sup>a</sup>, Marion Girard<sup>a</sup>, Cyril Lupi<sup>b</sup>, Dominique Leduc<sup>b</sup>, Frédéric Jacquemin<sup>a</sup>

<sup>1</sup>Institut de recherche en Génie Civil et Mécanique, GeM-E3M, UMR CNRS 6183, University of Nantes, France, 58 Rue Michel Ange 44600 Saint Nazaire

<sup>2</sup>Institut de recherche en Génie Civil et Mécanique, GeM-TRUST, UMR CNRS 6183, University of Nantes, France, 2 Chemin de la Houssinière 44300 Nantes

## **Abstract**

This article presents an application of a fiber optic sensor based on Fresnel reflection for the measurement of local water content within an epoxy adhesive immersed in water. The water content is directly calculated from the measured refractive index with the help of a Maxwell-Garnett model which consider spherical water inclusions inside an epoxy matrix. No calibration is needed. Three samples were equipped with fiber optic sensors and immersed in water. The measured water content was compared with a finite element simulation. The remarkable agreement between both validates the proposed method. In an industrial setting, this experimental approach could be used to monitor the aging of an immersed polymer material, bonded joint or composite structure.

## **Keywords**

Polymer material; Water diffusion; Fiber optic sensor; Aging monitoring; Non-destructive testing

## **1. Introduction**

There are several types of structural joints, the best known are welding, riveting/bolting and adhesive bonding. This last method offers the possibility to join different materials, and enables, without alteration of substrates (drilling, heating ...), a better distribution of the stresses which makes it possible to reduce the size (thus the weight) of the structural parts. Many studies are interested in the durability of bonded joint [1,2,3]. Indeed, bonding offers the possibility of

lightening structures and reducing production costs. But it is difficult to assess in service durability. This durability is questionable when these structures are subjected to aggressive environments (high humidity, immersion, high temperature, corrosive products ...). As structural adhesives are polymers, it is important to know their service environments. Indeed, the adhesive, a hydrophilic area by definition, controls the degradation modes of the structure. The hydrophilic nature of the adhesive [4] gives it the ability to absorb water (Fig. 1). To characterize this macroscopic water uptake, gravimetric tests are generally used [5-6]. This absorption can lead to a drop in mechanical properties and affect the durability of the structure [7].

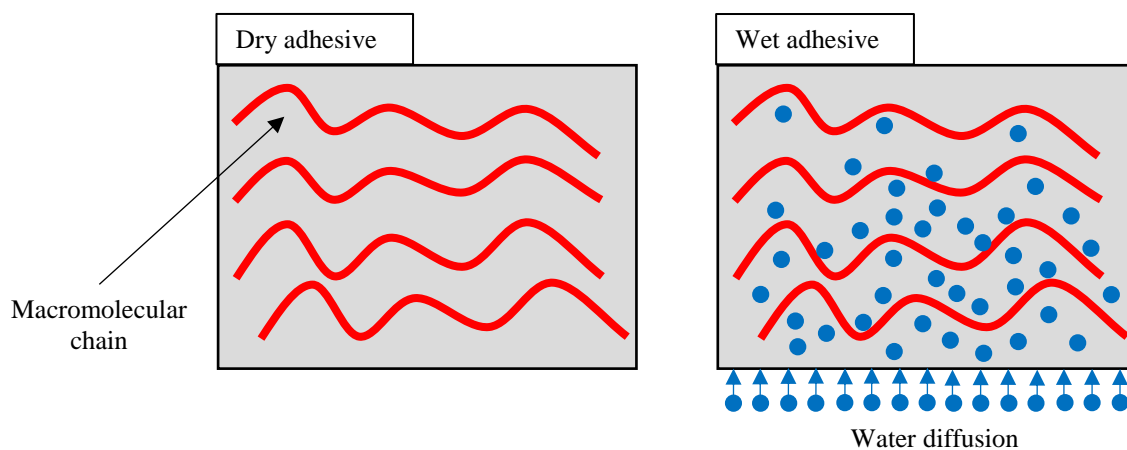


**Fig. 1.** Water diffusion in a polymer

So the water content is a key point parameter regarding the durability, but it has to be measured *in situ*. Fiber optic sensors seem to be an ideal candidate to perform such a monitoring. In the literature, studies [6,7] has already shown the ability of fiber Bragg gratings (FBG) to detect moisture contamination within a bonded structure. In these studies, the moisture is indirectly measured from the deformation it induces.

In our study, a fiber optic sensor based on Fresnel reflection was used and inserted into the core of the material. The sensor, which will be called a Fresnel sensor, allows the local measurement of the refractive index of a material. More precisely, the sensor probes a volume with a depth of the order of the wavelength around the end of the fiber. Aduriz (2007) [10] already used this

sensor to measure the polymerization rate of an epoxy resin and a previous study [11] also monitored the polymerization rate of the adhesive used.

In this work, we will only focus on the water diffusion. When the sample is immersed, the water diffuses in it and causes a structural change (molecular or compositional) [12]. The probed volume becomes a composite material made of water inclusions inside an epoxy matrix. This kind of material can be described by an effective refractive index in the framework of the Maxwell-Garnett model [13]. The only free parameter in the model is the water content. So it can easily be retrieved from the measurement of the refractive index. The aim of this study is to prove experimentally the validity of this approach.

## **2. Materials and methods**

### **2.1 Materials**

The polymer material used is an adhesive. In this study is a commercial two-component epoxy adhesive. It consists of an epoxy resin, a hardener based on modified amines and fillers particles. During processing, a chemical reaction occurs between the epoxy resin and the hardener. The industrial application of this study is the marine turbine structures. The bonding time of these large structures can be long (about a day). In this context, the first 24 hours curing phase under ambient conditions has been fixed. And then, a 24 hours post curing at 60 °C was performed to complete the crosslinking reaction. In conclusion, the manufacturing process is as follow: 24 h under ambient conditions followed by 24 h at 60 °C.

### **2.1 Gravimetric tests**

Polymer materials are hydrophilic and can absorb water, to characterize the water diffusion kinetics, gravimetric tests were carried out. For this purpose, discs specimens with a diameter of 70 mm and a thickness of 2 mm have been manufactured. These dimensions have been chosen to consider a 1D diffusion in the thickness  $z$  direction (thickness  $\ll$  diameter),  $z$  is between 0 and 2 mm (Fig. 2).

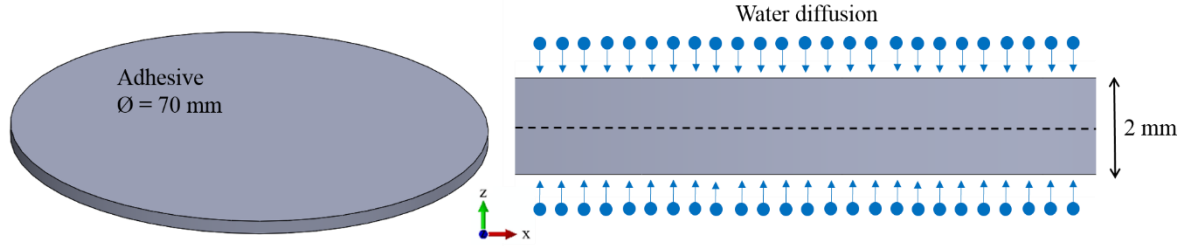


**Fig. 2.** An adhesive disc specimen

These specimens were immersed in water at 40 °C, and the mass was measured during the immersion. The water temperature has been set to accelerate the aging phenomena. The macroscopic water content  $C(t)$  that diffuses within the material can be calculated with the equation (1).

$$C(t) = \frac{m(t) - m_{t_0}}{m_{t_0}} \cdot 100 \quad (1)$$

Where  $m(t)$  represents the mass of the specimen during immersion and  $m_{t_0}$  the initial mass of the specimen before immersion.

## 2.2 Water diffusion and corresponding model

This water uptake depends on two parameters:  $D$  ( $\text{mm}^2 \cdot \text{s}^{-1}$ ) the diffusion coefficient which characterizes the water diffusion rate within the material, and  $C_{\text{sat}}$  (%) which characterizes the maximum water content in the material. To determine these two parameters, gravimetric tests consisting of monitoring the evolution of the mass of the material during immersion were carried out. In the literature, there are several water diffusion models, which are used to predict the water uptake of a material. The idea is to determine the evolution of the macroscopic water content of the material, noted  $C(t)$ , as a function of the square root of time. Weitsman (2012) [14] defined 6 main families of diffusion kinetics typical of polymer and polymer matrix composites. In this work, we will only focus on two of them. The most well-known diffusion model is the Fick model. A kinetics according to this model, called "fickian" (Fig. 3 – graph 1), is characterized by two distinct parts. In the first part, the water content increase linearly until

it reaches a level corresponding to saturation,  $C_{\text{sat}}$  of the material. It is common to see a diffusion gap compared to this model, it is what we will call a "non-fickian" diffusion kinetics (Fig. 3 – graph 2). After a rapid initial absorption of water, the water uptake remains continuous, although less important. Contrary to what the Fick model predicts, the material reaches saturation for much longer periods of time. This suggests that after a first phase of rapid diffusion of the order of a few days, a second, slower diffusion process occurs. This two-step moisture transport model has been successfully used to interpret aging tests when water diffusion shows an anomaly process [13,14].

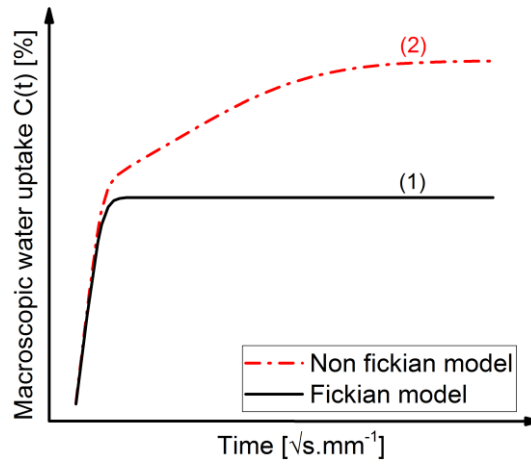


**Fig. 3.** Water diffusion kinetics model (fickian and non fickian)

For unidirectional diffusion in the  $z$  direction, the Fick model is:

$$\frac{\partial c(z, t)}{\partial t} = D \frac{\partial^2 c(z, t)}{\partial z^2} \quad (2)$$

Where the local water content  $c(z, t)$  is a function of space and time. Considering a thin plate of thickness  $e$  that initially does not contain moisture, there is an analytical solution to this problem given by Crank (1975) [17] to calculate the local water content for a given  $z$  position  $c(z, t)$ :

$$c(z, t) = c_{\text{sat}} \left( 1 - \frac{4}{\pi} \sum_{n=0}^{\infty} \frac{(-1)^n}{2n+1} \exp \left[ -D(2n+1)^2 \pi^2 \frac{t}{e^2} \right] \cos \left[ (2n+1) \pi \frac{z}{e} \right] \right) \quad (3)$$

By integrating on the volume, the macroscopic water content  $C(t)$  is:

$$C(t) = C_{\text{sat}} \left( 1 - \frac{8}{\pi^2} \sum_{n=0}^{\infty} \frac{1}{(2n+1)^2} \exp \left[ -D(2n+1)^2 \pi^2 \frac{t}{e^2} \right] \right) \quad (4)$$

As we will see later on this model is not suitable for the adhesive used, we used a Dual Fick model which consists of the sum of two Fick models (2).

$$\frac{\partial c_1(z, t)}{\partial t} + \frac{\partial c_2(z, t)}{\partial t} = D_1 \frac{\partial^2 c_1(z, t)}{\partial z^2} + D_2 \frac{\partial^2 c_2(z, t)}{\partial z^2} \quad (5)$$

This model considers two diffusion processes as shown in (Fig. 3 – graph 2): a first process characterized by a diffusion coefficient  $D_1$  and a saturation water content  $C_{\text{sat}1}$ , and a second characterized by  $D_2$  and  $C_{\text{sat}2}$ . Considering a thin plate of thickness  $e$  that initially does not contain moisture, the resolution of the equation (5) allows to calculate the local water content  $c(z, t)$ .

$$c(z, t) = \sum_{i=1}^2 \left[ C_{\text{sat}_i} \left( 1 - \frac{4}{\pi} \sum_{n=0}^{\infty} \frac{(-1)^n}{2n+1} \exp \left[ -D_i(2n+1)^2 \pi^2 \frac{t}{e^2} \right] \cos \left[ (2n+1) \pi \frac{z}{e} \right] \right) \right] \quad (6)$$

where  $D_i$  represents the diffusion coefficient,  $C_{\text{sat}_i}$  the water content at saturation,  $e$  the thickness of the sample and  $z$  the position in the thickness.

By integrating on the volume, the macroscopic water content  $C(t)$  is:

$$C(t) = \sum_{i=1}^2 \left[ C_{\text{sat}_i} \left( 1 - \frac{8}{\pi^2} \sum_{n=0}^{\infty} \frac{1}{(2n+1)^2} \exp \left[ -D_i(2n+1)^2 \pi^2 \frac{t}{e^2} \right] \right) \right] \quad (7)$$

### 2.3 Fiber optic sensor based on Fresnel reflection

Optical fiber is a glass or plastic wire that has the ability to conduct light. It generally consists of two concentric cylinders made of silica: the core and the cladding (Fig. 4).

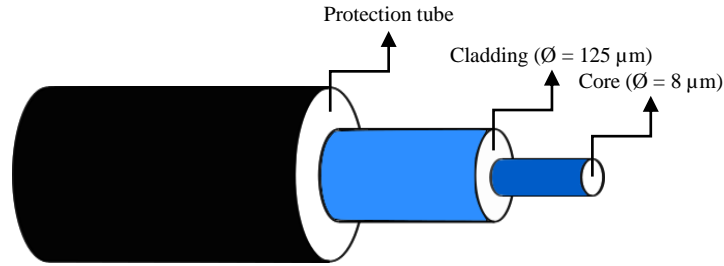


**Fig. 4.** Diagram of an optical fiber

The light spreads within the core. The optical fiber used in this study are single mode optical fiber (SMF28) with a core diameter of  $8\ \mu\text{m}$  and a cladding of  $125\ \mu\text{m}$  (produce from iXblue IXF-SM-1550-125). The refractive index is 1.457 at 1550 nm. By cleaving an optical fiber, and based on Fresnel reflection, it is possible to quantify the refractive index of a surrounding environment. The cleavage at the end of an optical fiber allows the creation of a diopter. According to *Snell-Descartes* laws, a part of incident light on the end of the fiber is reflected and provide a back reflection in the core of the fiber (Fig. 5).

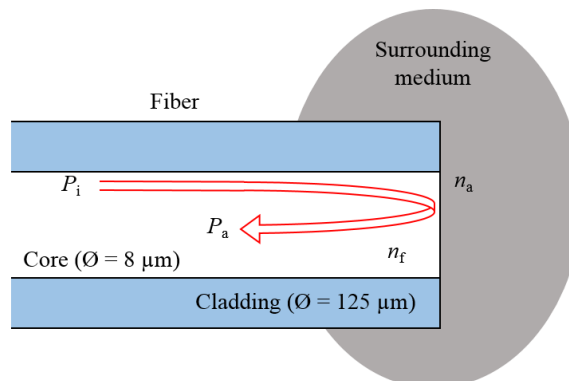


**Fig. 5.** Principle of the Fresnel sensor

In the literature, Cusano (2000) [18] proposes to determine the refractive index by measuring the reflected power by the sensor. A first one is done in a known environment (air for example) and the second one in the targeted environment (adhesive in our case of study). The two values of reflected power are then used in equation (8) to retrieve refractive index of the unknown environment:

$$n_a = -n_f \left( \frac{\eta + 1}{\eta - 1} \right) \quad \text{with} \quad \eta = \left( \frac{n_f - n_{\text{air}}}{n_f + n_{\text{air}}} \right) \left( \frac{P_a}{P_{\text{air}}} \right)^{\frac{1}{2}} \quad (8)$$

Where  $P_{\text{air}}$  is the reflected power when the sensor is in the air and  $P_a$  is the reflected power when the sensor is in the bonded joint. In this study, the air refractive index is considered equal to  $n_{\text{air}} = 1.000$  and the refractive index of the fiber is  $n_f = 1.457$ .

This sensor used allows to measure a refractive index on a cylinder of  $8 \mu\text{m}$  (diameter of the core of the optical fiber) and around  $1.55 \mu\text{m}$  deep (wavelength used). To make the measurement, a laser with  $1550 \text{ nm}$  wavelength is used. It is connected to a 2 by 1 optical coupler and the optical wave propagated through the coupler and then inside the optical fiber. The optical wave reflected by the sensor is then backscattered in the fiber and measured on a photo-receiver through the coupler. To interrogate this sensor, the setup includes (Fig. 6):

- A laser of low coherence ( $1550 \text{ nm}$ )
- An optical coupler
- A detector (photodiode + voltage acquisition system)

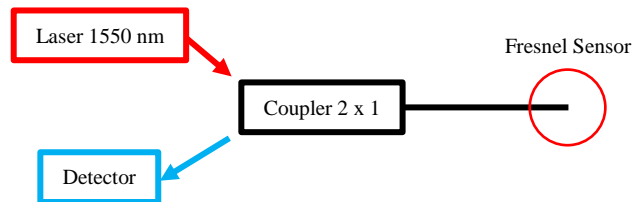


**Fig. 6.** Principle of measurement of Fresnel sensor

#### 2.4 Instrumentation of specimens by Fresnel sensor

A sensor was inserted into the core of a  $70 \text{ mm}$  diameter and  $2 \text{ mm}$  thickness disc (Fig. 7). To keep the sensor at the center of the disc, a 3D printing mold was developed and used. We ensured that this position is correct with post-mortem MEB analysis.

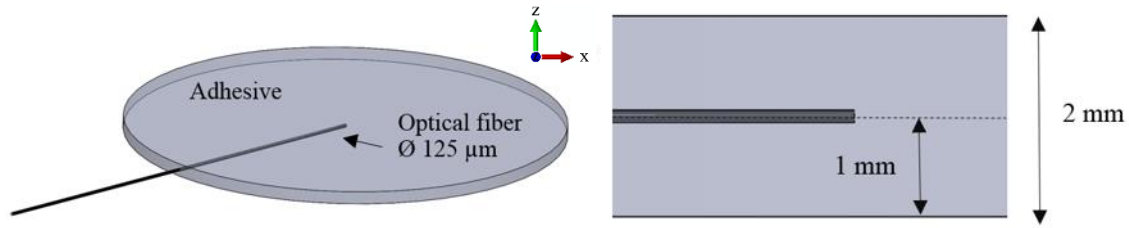


**Fig. 7.** Insertion of a Fresnel sensor into an adhesive disc specimen

After insertion of the sensor, the adhesive crosslinking was carried out: 24 h under ambient conditions followed by a post curing of 24 h at 60 °C. Following the polymerization reaction, the refractive index of the adhesive at 40 °C is  $n_0 = 2.904 \pm 0.002$  [11].

### 3. Results and discussions

First, gravimetric tests on adhesive discs were carried out to identify the diffusion parameters. Then, it is possible to calculate the local water content field. In parallel, refractive index measurements during immersion on specimens instrumented by Fresnel sensors were performed. The results will make it possible to prove an optical model to experimentally determine the local water content with refractive index measurements.

#### 3.1 Gravimetric tests

In order to determine the water diffusion kinetics of the adhesive, 12 discs of 70 mm diameter and 2 mm thickness were manufactured.

##### 3.1.1 Macroscopic results

These specimens, they were immersed in water at 40 °C. By measuring their mass during immersion, the macroscopic water content  $C(t)$  can be calculated. Measurements were made periodically according to the square root of time. The (Fig. 8) allows to know the water diffusion kinetics of the adhesive. Using the Dual-Fick model presented above, it is possible to calculate the diffusion parameters (Tab. 1) with the equation (7).

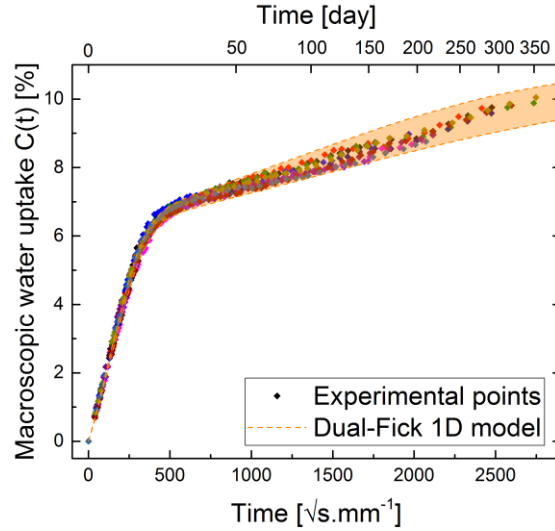


**Fig. 8.** Evolution of the macroscopic water uptake as a function of immersion time

$D_1$ [ $\text{mm}^2 \cdot \text{s}^{-1}$ ]	$(1.62 \pm 0.07) \cdot 10^{-6}$
$C_{\text{sat}1}$ [%]	$6.17 \pm 0.04$
$D_2$ [ $\text{mm}^2 \cdot \text{s}^{-1}$ ]	$(2.06 \pm 0.36) \cdot 10^{-8}$
$C_{\text{sat}2}$ [%]	$4.56 \pm 0.36$

**Tab. 1.** Identified parameters of the diffusive model used (Dual Fick)

An identification was performed on each specimen. The parameters in (Tab. 1) correspond to the mean and standard deviation on the 12 specimens. The difference observed between the specimens comes from the experimental dispersion. Now that the parameters of water diffusion in the adhesive are known, it is important to know the local water content  $c(z,t)$  present at the sensor level when it is inserted into a specimen (Fig. 7).

### 3.1.2 Local water content distributions - Simulation

To model the water content field, a finite element calculation simulation using the Abaqus<sup>TM</sup> software was performed. Thermal transfer functions are used to simulate water diffusion. Indeed, Yoon (2016) [19] shows that it is possible to make an analogy between the laws of Fourier and Fick. As shown in equation (5), the Dual-Fick model represents the sum of two Fick models. To simulate the Dual-Fick model, it is sufficient to perform two simulations, one with parameters  $D_1$  and  $C_{\text{sat}1}$  and the other with parameters  $D_2$  and  $C_{\text{sat}2}$  of (Tab. 1) and to add the water content fields. A quadratic 2D heat transfer elements (DC2D4) were used. For the

mesh, 143887 elements have been used and a higher mesh density was adopted for the element around the measurement area. The boundary conditions used are as follows:

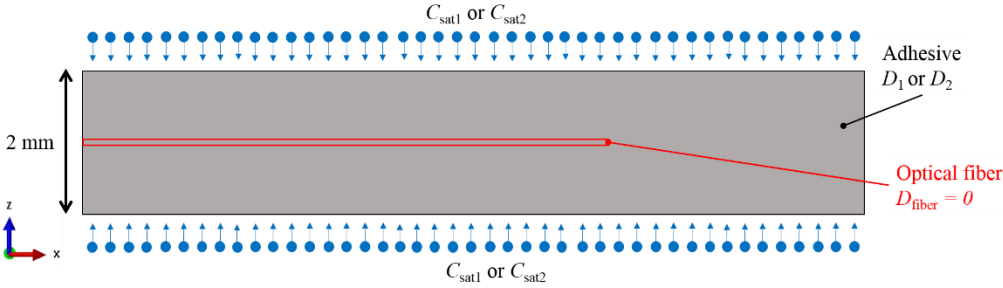


**Fig. 9.** Boundary conditions for the simulation of Dual-Fick model on an instrumented specimen

By implementing the parameters (Tab. 1) in the finite element calculation software Abaqus™ it is possible to know the evolution of the local water content field of the specimen for different immersion times (Fig. 10).

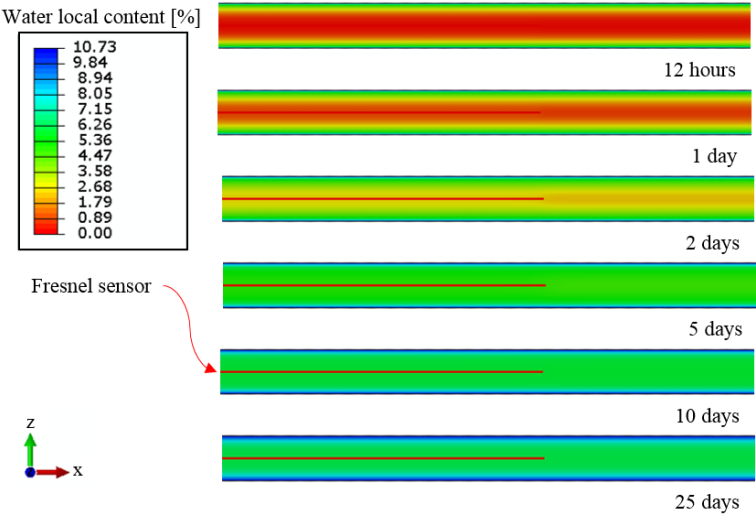


**Fig. 10.** Evolution of the water local content field for different immersion times

Results (Fig. 10) show the evolution of the local water content field for a specimen instrumented by a Fresnel sensor. As the optical fiber is hydrophobic, so there is no water diffusion inside the sensor. It is also possible to calculate the local water content using equation (6). The simulation make it possible to measure the evolution of the local water content  $c(z,t)$  at the end of the optical fiber and to compare with the analytical solution (Fig. 11).

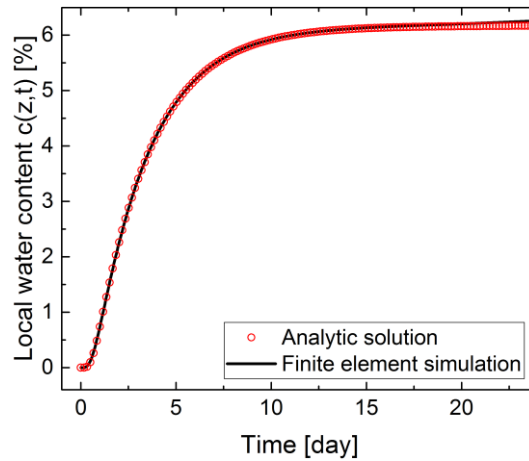


**Fig. 11.** Local water content as a function of immersion time at the sensor

The results (Fig. 11) shows the local water content at the sensor when measuring the refractive index during immersion. The results obtained by the analytic solution and the simulation are very close. A maximum deviation of 1.6% was calculated. In the following, we will only use the simulation results.

### 3.2 Refractive index measurement

Three instrumented specimens were immersed in water at 40 °C. The (Fig. 12) shows the evolution of the refractive index measured by Fresnel sensors during immersion.

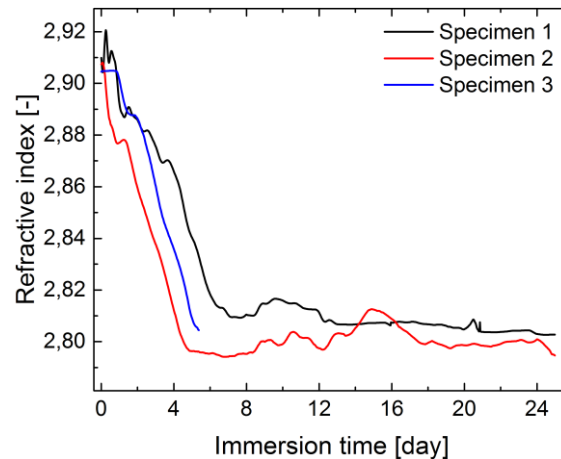


**Fig. 12.** Evolution of the refractive index for instrumented specimens as a function of immersion time

The results obtained (Fig. 12) allows to highlight a drop in the refractive index of the adhesive during immersion. The curves can be divided into two parts. The first part (under 6 days) shows a significant drop in the refractive index. The second part seems to show a stabilization of this refractive index. For specimen 3, reflected power variations were observed between 6 and 14

days. The variations are due to the evolution of the light incident on the sensor due to a change in the position of the optical fiber between the laser and the specimen during the test (curve or movement of the fiber). In the model used we need the initial incident light to determine the refractive index, for specimen 3 after 6 days the model is therefore no longer valid. We decided not to calculate the refractive index of specimen.

### 3.3 Refractive index model

#### 3.3.1 Theoretical model

When water diffuses into the adhesive, the material becomes a composite material consisting of water inclusions in the epoxy adhesive. There are several models that can be used to estimate the refractive index of a composite material. In the case of low concentrations and for approximately spherical inclusions, the Maxwell-Garnett model [20] is well adapted. We will use here the formalism defined by Markel (2006) [13] :

$$n_{a/w}(t) = n_a \sqrt{\frac{1 + 2f(t) \frac{n_w^2 - n_a^2}{n_w^2 + 2n_a^2}}{1 - f(t) \frac{n_w^2 - n_a^2}{n_w^2 + 2n_a^2}}} \quad (9)$$

With  $n_{a/w}(t)$  the refractive index of the adhesive/water system which depends on the immersion time,  $n_a$  the refractive index of the adhesive ( $n_a = 2.904$ ),  $n_w$  the refractive index of the water ( $n_w = 1.333$ ) and  $f(t)$  the volume fraction of water. Using equation (9) and measuring the refractive index of the the adhesive/water system, it is then possible to calculate the volume fraction  $f(t)$  of the water.

#### 3.3.2 Water volume fraction

The evolution of the volume fraction of water  $f(t)$  can be calculated by the following equation:

$$f(t) = \frac{V_w(t)}{V_a} = \frac{c(z, t) \cdot m_{t0}}{V_a \cdot \rho_w} \quad (10)$$

With  $V_w(t)$  the water volume,  $V_a$  the adhesive volume,  $m_{t0}$  the mass of the adhesive before immersion,  $\rho_w$  the density of water and  $c(z,t)$  the local water content. With the results (Fig. 11), it is then possible to plot the evolution of the volume fraction of water in front of the sensor during the immersion.

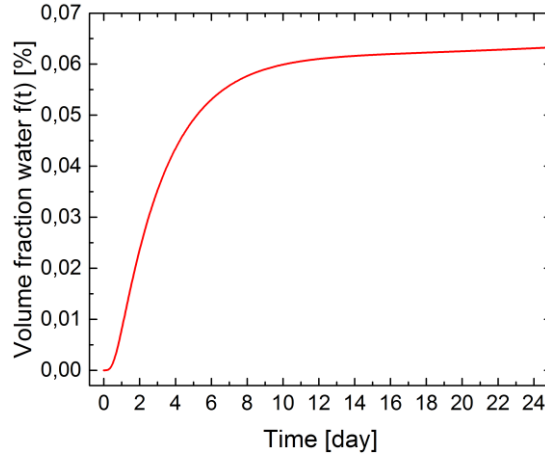


**Fig. 13.** Volume fraction of water as a function of immersion time at the sensor

### 3.3.3 Theoretical evolution of the refractive index during immersion

The refractive index measured in (Fig. 12) corresponds to  $n_{a/w}(t)$  of the equation (9). It is possible to determine the local water content as a function of the refractive index  $n_{a/w}(t)$  using the equations (9) and (10).

$$c(z, t) = \left( \frac{V_a \cdot \rho_w}{m_{t0}} \right) \cdot \left( \frac{n_{a/w}^2(t) - n_a^2}{n_w^2 - n_a^2} \right) \cdot \left( \frac{n_w^2 + 2n_a^2}{n_{a/w}^2(t) + 2n_a^2} \right) \quad (11)$$

Using the equation of the refractive index model (11), the equation (9) and the results of (Fig. 13), the theoretical refractive index depends on the local water content.

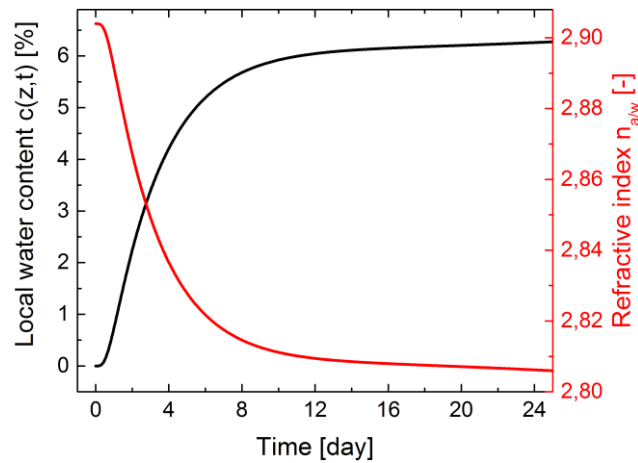


**Fig. 14.** Evolution of local water content and refractive index as a function of immersion time

### 3.3.4 Determination of the local water content with the refractive index measurement of the adhesive

The optical model (11) allows the local water content to be calculated using experimental refractive index measurements (Fig. 12). It is then possible to compare them with the analytical solution determined using gravimetric tests and Dual Fick model (Fig. 11).

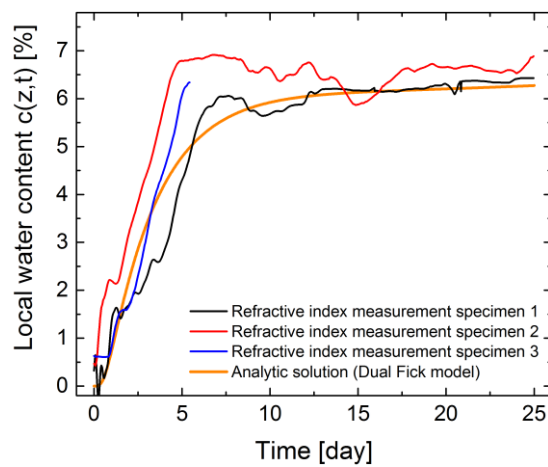


**Fig. 15.** Evolution of the refractive index as a function of immersion time (experimental results with refractive index model and analytic solution with Dual Fick model)

During the first 6 days of immersion the local water content of the adhesive increases significantly. Then it stabilizes after 10 days. A comparison between the results obtained by measuring the refractive index with the analytical solution of the Dual Fick model was carried out. During the first 10 days, when the local water content increases, an average deviation between two models is 13 %. Between 10 and 25 days, when the stabilization of the local water

content, the average deviation decreases at 4%. In conclusion, the optical model of water inclusions represents the behavior of the local water content (Fig. 15).

To note the Dual-Fick model provides for a second phase of much slower water diffusion, which could be translated into a slow decrease in the refractive index. In this study, the time duration of the tests was too short to observe this second process.

### 3.3.5 Link between refractive index and local water content

With results (Fig. 12) and (Fig. 15) the refractive index of the adhesive can be related to its local water content (Fig. 16). An average and a standard deviation on the three instrumented specimens was calculated.

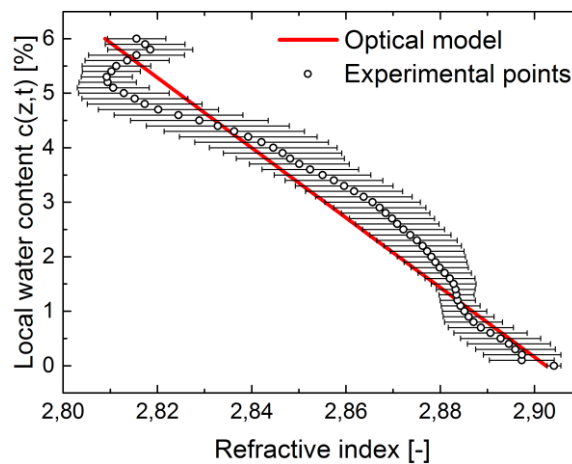


**Fig. 16.** Variation of the refractive index according to the local water content

The results (Fig. 16) show a dependence between the refractive index and the local water content. The experimental points follow the optical model of the equation (11). It is therefore possible with the Fresnel sensor to measure the local water content in the core of a material by measuring the refractive index.

## 4. Conclusion

This study shows the possibility of measuring the local water content of an epoxy-amine adhesive using a refractive index measurement. For this purpose, a fiber optic sensor based on Fresnel reflection was used. This sensor allows an *in situ* and non-destructive measurement of

the local water content. To our knowledge, this makes it the first *in situ* water sensor at the heart of a material. It is also important to note that this optical measurement method is easy to use. In industrial context, this sensor would allow a follow-up of the health of a bonded joint or composite structure in immersion.

### Acknowledgement

This study is part of the INDUSCOL project and the authors wish to associate the industrial partner of this project; Naval Group. This work benefited from France Energies Marines and State financing managed by the National Research Agency under the Investments for the Future program bearing the reference ANR-10-IED-0006-08.



ANR-10-IED-0006-08

### Bibliography

- [1] J. M. Sousa, J. R. Correia, and S. Cabral-Fonseca, “Durability of an epoxy adhesive used in civil structural applications,” *Constr. Build. Mater.*, vol. 161, pp. 618–633, 2018.
- [2] M. Heshmati, R. Haghani, and M. Al-Emrani, “Environmental durability of adhesively bonded FRP/steel joints in civil engineering applications: State of the art,” *Compos. Part B Eng.*, vol. 81, pp. 259–275, 2015.
- [3] C. Mandolfino, E. Lertora, C. Gambaro, and M. Pizzorni, “Durability of polyamide bonded joints: influence of surface pre-treatment,” *Int. J. Adhes. Adhes.*, vol. 86, no. August, pp. 123–130, 2018.
- [4] H. Träubel, *New Materials Permeable to Water Vapor*. 1999.
- [5] X. Han, Y. Jin, W. Zhang, and W. Hou, “Characterisation of moisture diffusion and strength degradation in an epoxy-based structural adhesive considering a post-curing process,” *J. Adhes. Sci. Technol.*, no. February 2019, 2018.
- [6] Y. C. Lin and X. Chen, “Moisture sorption-desorption-resorption characteristics and its effect on the mechanical behavior of the epoxy system,” *Polymer (Guildf.)*, vol. 46, 2005.
- [7] A. D. Crocombe, Y. X. Hua, W. K. Loh, M. A. Wahab, and I. A. Ashcroft, “Predicting the residual strength for environmentally degraded adhesive lap joints,” *Int. journal Adhes. Adhes.*, vol. 26, pp. 325–336, 2006.
- [8] M. Mieloszyk and W. Ostachowicz, “Moisture contamination detection in adhesive bond using embedded FBG sensors,” *Mech. Syst. Signal Process.*, vol. 84, pp. 1–14, 2017.
- [9] V. Bonilla, M. Mieloszyk, and W. Ostachowicz, “Model of moisture absorption by adhesive joint,” *Mech. Syst. Signal Process.*, vol. 99, pp. 534–549, 2018.

- [10] X. A. Aduriz, C. Lupi, N. Boyard, J. Bailleul, D. Leduc, and V. Sobotka, “Quantitative control of RTM6 epoxy resin polymerisation by optical index determination,” *Compos. Sci. Technol.*, vol. 67, pp. 3196–3201, 2007.
- [11] R. Grangeat, M. Girard, C. Lupi, D. Leduc, and F. Jacquemin, “Revealing of interphases in bonded joints with a fiber optic sensor based on Fresnel reflection,” *Int. J. Adhes. Adhes.*, vol. 91, no. February, pp. 12–18, 2019.
- [12] K. M. Davis and M. Tomozawa, “Water diffusion into silica glass: Structural changes in silica glass and their effect on water solubility and diffusivity,” *J. Non. Cryst. Solids*, vol. 185, no. 3, pp. 203–220, 1995.
- [13] V. A. Markel, “Introduction to the Maxwell Garnett approximation: tutorial,” *J. Opt. Soc. Am. A*, vol. 33, no. 7, p. 1244, 2016.
- [14] Y. J. Weitsman, *Fluid Effects in Polymers and Polymeric Composites*. 2012.
- [15] W. K. Loh, A. D. Crocombe, M. M. A. Wahab, and I. A. Ashcroft, “Modelling anomalous moisture uptake, swelling and thermal characteristics of a rubber toughened epoxy adhesive,” *Int. J. Adhes. Adhes.*, vol. 25, no. 1, pp. 1–12, 2005.
- [16] M. D. Placette, X. Fan, and D. Edwards, “A dual stage model of anomalous moisture diffusion and desorption in epoxy mold compounds,” *2011 12th Intl. Conf. Therm. Mech. Multi-Physics Simul. Exp. Microelectron. Microsystems*, p. 1/8-8/8, 2011.
- [17] J. Crank, *The Mathematics of Diffusion*. 1975.
- [18] A. Cusano, “Optoelectronic sensor for cure monitoring in thermoset-based composites,” *Sensors Actuators, A Phys.*, vol. 84, no. 3, pp. 270–275, 2000.
- [19] S. Yoon, B. Han, and Z. Wang, “On Moisture Diffusion Modeling Using Thermal-Moisture Analogy,” vol. 129, no. December 2007, pp. 421–426, 2016.
- [20] J. C. M. Garnett, “Colours in Metal Glasses and in Metallic Films,” vol. 203, pp. 385–420, 1904.